

Facile Ru-Ru Bond Cleavage and Reformation in a Pentanuclear Carbonyl Cluster: Synthesis and X-ray Structural Studies of $\text{Ru}_5(\text{CO})_{13}(\mu_4\text{-}\eta^2\text{-C}\equiv\text{CPh})(\mu\text{-PPh}_2)$ and Its CO Adduct $\text{Ru}_5(\text{CO})_{14}(\mu_5\text{-}\eta^2\text{-C}\equiv\text{CPh})(\mu\text{-PPh}_2)$

Shane A. MacLaughlin, Nicholas J. Taylor, and Arthur J. Carty*

Guelph-Waterloo Centre for Graduate Work in Chemistry, Waterloo Campus, University of Waterloo, Waterloo, Ontario N2L 3G1

Received February 22, 1983

The pentanuclear ruthenium cluster $\text{Ru}_5(\text{CO})_{13}(\mu_4\text{-}\eta^2\text{-C}\equiv\text{CPh})(\mu\text{-PPh}_2)$ (I) has been synthesized by thermolysis of $\text{Ru}_3(\text{CO})_{11}(\text{Ph}_3\text{PC}\equiv\text{CPh})$. Crystals of I are monoclinic of space group $P2_1/n$, with $a = 9.966$ (2) Å, $b = 16.877$ (2) Å, $c = 21.707$ (4) Å, $\beta = 100.51$ (2)°, $Z = 4$, $R = 0.033$, and $R_w = 0.039$ for 3335 observed, diffractometer measured reflections. The cluster has a square-pyramidal array of metal atoms with a phosphido bridge across a basal edge ($\text{Ru}(4)\text{-Ru}(5) = 2.696$ (1) Å; $\text{Ru}(4)\text{-P-Ru}(5) = 72.3$ (0)°) and a $\mu_4\text{-}\eta^2\text{-acetylidyne}$ bridging the basal face. The acetylidyne carbon atom C(14) resembles the carbido carbon atom in the related structure $\text{Ru}_5(\text{CO})_{15}\text{C}$. The reaction of I with CO affords a new cluster, $\text{Ru}_5(\text{CO})_{14}(\mu_5\text{-}\eta^2\text{-C}\equiv\text{CPh})(\mu\text{-PPh}_2)$ (II), which has also been structurally characterized by X-ray diffraction. Crystals of II are monoclinic of space group $P2_1/n$ with $a = 17.818$ (3) Å, $b = 12.099$ (2) Å, $c = 19.435$ (3) Å, $\beta = 115.95$ (2)°, and $Z = 4$. The structure was solved by heavy-atom methods and refined to R and R_w values of 0.033 and 0.037. Addition of CO to I causes an opening of a basal Ru-Ru bond; II consists of three Ru_3 triangles sharing two sides. This skeletal rearrangement is accompanied by a change in acetylidyne-cluster bonding with the unsaturated ligand attached to all five ruthenium atoms via a $\mu_5\text{-}\eta^2$ mode. The addition of CO to I is reversible. Other Lewis bases, MeCN, PhCN, *i*-PrNH₂, *sec*-BuNH₂, and C₆H₅N, also add reversibly to I giving adducts which have been studied by IR and ³¹P NMR spectroscopy. The reversible cleavage of an Ru-Ru bond in I is discussed in terms of reactivity patterns for metal clusters.

Introduction

The potential catalytic activity of polynuclear transition-metal clusters,¹ currently of great interest, implies the operation of certain activating mechanisms, particularly the introduction of coordinative unsaturation. Though in mononuclear systems this unsaturation is usually explicit,² formally saturated multinuclear metal-metal bonded systems may mimic the behavior of unsaturated systems through uptake of a substrate with concomitant metal-metal bond cleavage.³ During this process polynuclear integrity of the cluster must be maintained. Unfortunately, however, the conditions under which this behavior might be observed often lead to cluster fragmentation⁴ and few examples of reversible metal-metal bond cleavage are known.⁵⁻⁹ Although significant changes in skeletal stereochemistry and ligand coordination might be expected to accompany metal-metal bond rupture in a polynuclear cluster, little is known of such rearrangements and our

understanding of how such changes influence ligand reactivity is in its infancy.

We have discovered several novel examples of reversible metal-metal bond cleavage involving the pentanuclear cluster $\text{Ru}_5(\text{CO})_{13}(\mu_4\text{-}\eta^2\text{-C}\equiv\text{CPh})(\mu\text{-PPh}_2)$ (I) which provide some insight into the extent of structural reorganization which may accompany Lewis base attack on a polynuclear carbonyl. In this paper we present full synthetic and structural details for the acetylidyne complex I¹⁰ and its CO adduct $\text{Ru}_5(\text{CO})_{14}(\mu_5\text{-}\eta^2\text{-C}\equiv\text{CPh})(\mu\text{-PPh}_2)$ (II) which is formed via cleavage of a single Ru-Ru bond in the precursor. The equilibrium nature of the relationship between I and II as well as between I and other Lewis base adducts has been demonstrated by ³¹P NMR spectroscopy. Conversion of I to II results in a dramatic skeletal rearrangement from a square-pyramidal Ru_5 core to an open "swallowlike" array of three triangles sharing two edges. This structural rearrangement converts a μ_4 -bound acetylidyne in I to a μ_5 ligand in II; as a result the α -carbon atom of the acetylidyne in II is significantly less exposed than in I. These changes may have important ramifications for the reactivity of multisite bound ligands in metal clusters.

Experimental Section

General Procedures. All manipulations were carried out under a blanket of high purity nitrogen by using Schlenk tube and stainless-steel transfer techniques. Solvents were dried over sodium benzophenone ketyl or LiAlH₄ and distilled under N₂ prior to use. Column chromatography utilized Baker "Florisil" (100–200 mesh). Infrared spectra were recorded on a Perkin-Elmer 180 spectrophotometer. NMR spectra were measured on Bruker WP-80 (³¹P) and WH-400 (South Western Ontario Regional High Field NMR Centre (GWC),² Guelph Campus) (¹³C). Deuterated solvents provided the ²D lock. Shifts are reported relative to external 85% H₃PO₄ (³¹P) and Me₄Si (¹³C).

(1) (a) Muetterties, E. L. *Science (Washington, D.C.)* 1977, 196, 839. (b) Thomas, M. G.; Beier, B. F.; Muetterties, E. L. *J. Am. Chem. Soc.* 1976, 98, 1296. (c) Muetterties, E. L.; Stein, J. *Chem. Rev.* 1979, 79, 479.

(2) See, for example: Cotton, F. A.; Wilkinson, G. "Advanced Inorganic Chemistry", 4th ed.; Wiley: New York, 1980.

(3) Johnson, B. F. G.; Lewis, J. *Adv. Inorg. Chem. Radiochem.* 1981, 24, 225.

(4) Chini, P.; Longoni, G.; Albano, V. G. *Adv. Organomet. Chem.* 1976, 14, 285.

(5) Recent examples include binuclear compounds,⁶ trinuclear clusters,⁷ tetrานuclear mixed clusters,⁸ and a pentanuclear system.⁹

(6) (a) Langenbach, H. J.; Vahrenkamp, H. *Chem. Ber.* 1979, 112, 3390, 3773. (b) Langenbach, H. J.; Keller, E.; Vahrenkamp, H. J. *Organomet. Chem.* 1979, 171, 259. (c) Roberts, D. A.; Mercer, W. C.; Zuhurak, S. M.; Geoffroy, G. L.; Debrasse, C. W.; Cass, M. E.; Pierpont, C. G. *J. Am. Chem. Soc.* 1982, 104, 910.

(7) (a) Huttner, G.; Schneider, J.; Miller, H. D.; Mohr, G.; von Seyerl, J.; Wohlfahrt, L. *Angew. Chem., Int. Ed. Engl.* 1979, 18, 76. (b) Carty, A. J.; MacLaughlin, S. A.; Taylor, N. J. J. *Organomet. Chem.* 1981, 204, C27. (c) Lesch, D. A.; Rauchfuss, T. B. *Organometallics* 1982, 1, 499.

(8) Richter, F.; Vahrenkamp, H. *Organometallics* 1982, 1, 756.

(9) Johnson, B. F. G.; Lewis, J.; Nicholls, J. N.; Oxton, I. A.; Raithby, P. R.; Rosales, M. J. *J. Chem. Soc., Chem. Commun.* 1982, 289.

(10) A preliminary account of a part of this work has appeared: Carty, A. J.; MacLaughlin, S. A.; Taylor, N. J. J. *Am. Chem. Soc.* 1981, 103, 2456.

Synthesis of $\text{Ru}_5(\text{CO})_{13}(\mu_4\text{-}\eta^2\text{-C}\equiv\text{CPh})(\mu\text{-PPh}_2)$ (I). $\text{Ru}_5(\text{CO})_{11}(\text{Ph}_2\text{PC}\equiv\text{CPh})^7$ (1.0 g) was refluxed in *n*-heptane for 6–8 h with a stream of dry nitrogen bubbling through the solution. Evaporation of the mixture afforded a blue-black precipitate which was separated by filtration. A $\nu(\text{CO})$ spectrum of the precipitate showed it to be a mixture of $\text{Ru}_3(\text{CO})_{12}$ and I. $\text{Ru}_3(\text{CO})_{12}$ can be removed by three methods. (a) Sublimation: the precipitate was vacuum sublimed at 80 °C for 3–4 h, yielding $\text{Ru}_3(\text{CO})_{12}$. The desired product I remained in the residue, which was dissolved in THF. To this solution was added 2–3 g of Florisil. The solvent was evaporated, and the Florisil mixture was dried in vacuo for 2 h. The coated support was then placed on a short Florisil column and elution with hexane under N_2 removed any residual $\text{Ru}_3(\text{CO})_{12}$ as a yellow band. The product could then be eluted with benzene or toluene. Evaporation of the eluant followed by addition of *n*-hexane or *n*-heptane precipitated I. (b) Chromatography: as in a above but without sublimation. Large amounts of $\text{Ru}_3(\text{CO})_{12}$ present may require substantial volumes of eluting solvent, with a consequent reduction in yields. (c) Derivatization: the precipitate was suspended in benzene under a moderate stream of CO, leaving solid $\text{Ru}_3(\text{CO})_{12}$ and $\text{Ru}_5(\text{CO})_{14}(\mu_5\text{-}\eta^2\text{-C}\equiv\text{CPh})(\mu\text{-PPh}_2)$ in solution. The solution was filtered under CO and evaporated, yielding I. Further purification could be performed as in a above. The total yield is approximately 30%: IR $\nu(\text{CO})$ (C_6H_{12}) 2076 (m), 2043 (vs), 2024 (s), 2014 (m), 2000 (w) cm^{-1} ; mp 214–216 °C; ^{31}P NMR (C_6D_6) δ +254 (263 K). Anal. Calcd: C, 34.29; H, 1.31; P, 2.68. Found: C, 34.62; H, 1.35; P, 2.68.

Synthesis of $\text{Ru}_5(\text{CO})_{13}(\mu\text{-CO})(\mu_5\text{-}\eta^2\text{-C}\equiv\text{CPh})(\mu\text{-PPh}_2)$ (II). $\text{Ru}_5(\text{CO})_{13}(\mu_4\text{-}\eta^2\text{-C}\equiv\text{CPh})(\mu\text{-PPh}_2)$ was dissolved in THF with vigorous stirring under a moderate stream of CO. The dark green solution rapidly turned red/brown (1–2 min to completion). Removal of the CO atmosphere yielded I. No decomposition of the cluster was observed during this process. Owing to the lability of the CO adduct in solution in the absence of a CO atmosphere conventional purification techniques such as vacuum evaporation and chromatography were not useful.

Solid crystalline samples of II were obtained by repeating the experiment in *n*-heptane to obtain a saturated solution of the adduct. This solution was filtered under CO and placed in a Schlenk tube under slightly more than 1 atm of CO. Storage at –10 °C for 1 week yielded brown-red crystals of $\text{Ru}_5(\text{CO})_{13}(\mu\text{-CO})(\mu_5\text{-}\eta^2\text{-C}\equiv\text{CPh})(\mu\text{-PPh}_2)$ (II). The molecule was completely characterized by single-crystal X-ray diffractometry (vide infra): IR ($\nu(\text{CO})$, C_6H_{12}) 2091 (m), 2067 (s), 2047 (s), 2024 (vs), 2017 (m), 2013 (m), 1998 (m), 1986 (w), 1848 (w br); ^{31}P NMR (THF/CDCl_3 , 1:1) δ +258.0 (263 K).

Synthesis of Derivatives $\text{Ru}_5(\text{CO})_{13}(\text{C}\equiv\text{CPh})(\text{PPh}_2)(\text{L})$ ($\text{L} = \text{MeCN, PhCN, C}_5\text{H}_5\text{N, }i\text{-PrNH}_2, \text{sec-BuNH}_2$). Solutions were prepared by suspending $\text{Ru}_5(\text{CO})_{13}(\mu_4\text{-}\eta^2\text{-C}\equiv\text{CPh})(\mu\text{-PPh}_2)$ (I 200 mg) in benzene (20 mL) followed by addition of a large (~10-fold) excess of nucleophile to yield red-brown solutions as I dissolved. Solid samples were obtained by rapid evaporation of solutions of I in a 50:50 mixture of THF and nucleophile. Solutions decomposed slowly (48 h) on standing, but solids were air stable. Attempted dissolution in heptane or benzene gave red-brown solutions which rapidly precipitated I. IR spectra were obtained by preparing a solution of nucleophile in cyclohexane ($\text{L} = \text{C}_6\text{H}_5\text{N, }i\text{-PrNH}_2, \text{sec-BuNH}_2$) or chloroform ($\text{L} = \text{MeCN, PhCN}$) for use in both sample and reference cells, with I in the sample cell.

$\text{Ru}_5(\text{CO})_{13}(\text{C}\equiv\text{CPh})(\text{PPh}_2)(\text{MeCN})$: IR $\nu(\text{CO})$ ($\text{CHCl}_3/\text{MeCN}$, 4:1) 2055 (s), 2041 (s), 2026 (vs), 1996 (vs br), 1961 (sh), 1935 (sh), 1831 (w, br); ^{31}P NMR (THF/CDCl_3 1:1) δ +258.2 (263 K). Anal. Calcd: C, 35.15; H, 1.51; Found: C, 35.85; H, 1.71.

$\text{Ru}_5(\text{CO})_{13}(\text{C}\equiv\text{CPh})(\text{PPh}_2)(i\text{-PrNH}_2)$: IR $\nu(\text{CO})$ ($\text{C}_6\text{H}_{12}/i\text{-PrNH}_2$, 6:1) 2056 (m), 2048 (s), 2028 (s), 2002 (s), 1992 (s), 1983 (s), 1958 (s), 1932 (sh), 1906 (w, sh), 1830 (w, br); ^{31}P NMR (THF/CDCl_3 , 1:1) δ +233 (315 K). Anal. Calcd: C, 35.62; H, 1.99. Found: C, 35.41; H, 2.05.

$\text{Ru}_5(\text{CO})_{13}(\text{C}\equiv\text{CPh})(\text{PPh}_2)(\text{sec-BuNH}_2)$: IR $\nu(\text{CO})$ ($\text{C}_6\text{H}_{12}/\text{sec-BuNH}_2$ 10:1) 2057 (m), 2048 (m), 2029 (s), 2004 (s), 1995 (s), 1976 (m), 1959 (s), 1948 (m, sh), 1924 (w), 1830 (w, br); ^{31}P NMR (THF/CDCl_3 1:1) δ +245 (293 K). Anal. Calcd: C, 36.19; H, 2.05. Found: C, 35.93; H, 3.38.

$\text{Ru}_5(\text{CO})_{13}(\text{C}\equiv\text{CPh})(\text{PPh}_2)(\text{C}_5\text{H}_5\text{N})$: IR $\nu(\text{CO})$ ($\text{C}_6\text{H}_{12}/\text{C}_5\text{H}_5\text{N}$, 10:1) 2058 (s), 2031 (vs), 2002 (s), 1992 (s), 1978 (m), 1962 (m), 1928 (w), 1910 (w, sh), 1820 (w, br); ^{31}P NMR (THF/CDCl_3

Table I. Crystallographic Data for X-ray Diffraction Studies

	$\text{Ru}_5(\text{CO})_{13}^-(\text{C}\equiv\text{CPh})(\text{PPh}_2)$	$\text{Ru}_5(\text{CO})_{14}^-(\text{C}\equiv\text{CPh})(\text{PPh}_2)$
formula	$\text{C}_{33}\text{H}_{15}\text{O}_{13}\text{PRu}_5$	$\text{C}_{34}\text{H}_{15}\text{O}_{14}\text{PRu}_5$
mol wt, g mol ⁻¹	1155.80	1183.81
space group	$\text{P}2_1/n$	$\text{P}2_1/n$
<i>a</i> , Å	9.966 (2)	17.818 (3)
<i>b</i> , Å	16.877 (2)	12.099 (2)
<i>c</i> , Å	21.707 (4)	19.435 (3)
β , deg	100.51 (2)	115.95 (2)
<i>V</i> , Å ³	3590 (1)	3767 (1)
<i>Z</i>	4	4
ρ_{calcd} g cm ⁻³	2.139	2.087
ρ_{measd} g cm ⁻³	2.14	2.08
$\mu(\text{Mo K}\alpha)$ cm ⁻¹	21.15	20.20
λ , Å	0.710 69	0.710 69
<i>F</i> (000)	2208	2264

1:1) δ +245 (293 K). Anal. Calcd: C, 36.99; H, 1.63. Found: C, 37.14; H, 2.27.

Reaction of I with PhCN gave a reddish brown solid which decomposed on pumping overnight in vacuo: IR spectra ($\nu(\text{CO})$ ($\text{CHCl}_3/\text{PhCN}$, 1:2) 2052 (m), 2038 (m, br), 2023 (s), 1990 (s), 1970 (sh, s), 1925 (m, br), 1818 (m, br)) confirmed the formation of an adduct similar to those above.

X-ray Structure Determinations. Collection and Reduction of X-ray Data. $\text{Ru}_5(\text{CO})_{13}(\text{C}\equiv\text{CPh})(\text{PPh}_2)$ (I). Blue-black crystals were grown from $\text{C}_7\text{H}_{16}/\text{C}_6\text{H}_6$ solutions at –10 °C. A crystal of dimensions 0.20 × 0.15 × 0.16 mm was attached to a glass fiber, mounted on a goniometer, and centered on a Syntex $\text{P}2_1$ fully automated four-circle diffractometer. The unit cell was determined from 15 randomly distributed reflections by using the Syntex autoindexing and cell refinement routines. Details are given in Table I. Intensity data were collected at 294 ± 1 K using Mo K α radiation monochromated via single-crystal graphite. A θ –2 θ scan mode with variable scan speeds of 2.0–29.3° min⁻¹ chosen to optimize measurements of weak reflections was used. Each scan had width from 0.8° below $\text{K}\alpha_1$ to 0.8° above $\text{K}\alpha_2$. Background counts using the stationary counter–stationary crystal routine were made at the beginning and end of each scan for a time equal to half of the scan time. The intensities of two standard reflections (109; 341) were monitored after every 100 reflections; only minor fluctuations in intensity were notable. Data were corrected for Lorentz and polarization effects but not absorption ($\mu(\text{Mo K}\alpha) = 21.15 \text{ cm}^{-1}$). From a total of 4721 independent reflections measured ($2\theta \leq 45^\circ$), 3335 with intensities $I \geq 3\sigma(I)$ were considered observed and used in the structure solution and refinement.

$\text{Ru}_5(\text{CO})_{14}(\text{C}\equiv\text{CPh})(\text{PPh}_2)$ (II). Initially a red-brown crystal grown from a dilute *n*-heptane solution at –10 °C was subjected to X-ray analysis. A 0.2-mm³ crystal, cut from a rod, was mounted on a glass fiber and coated with a layer of epoxy cement to minimize loss of carbon monoxide. A monoclinic unit cell of apparent dimensions $a = 9.636$ (1) Å, $b = 22.585$ (3) Å, $c = 10.253$ (2) Å, and $\beta = 115.27$ (1) Å of volume 2018.2 (5) Å³ was refined by using the Syntex autoindexing procedure. With $Z = 2$ and $\rho_{\text{measd}} = 2.01 \text{ g cm}^{-3}$ ($\rho_{\text{calcd}} = 2.030 \text{ g cm}^{-3}$) the calculated molecular weight corresponded to the formula $\text{Ru}_5(\text{CO})_{14}(\text{C}_2\text{Ph})(\text{PPh}_2) \cdot 0.5\text{C}_7\text{H}_{16}$. Intensity data were collected for what appeared to be a $\text{P}2_1$ (or $\text{P}2_1/m$) cell. The structure was solved by using MUL-TAN. Initial refinement revealed an apparent mirror disorder which was accommodated by refining the structure in $\text{P}2_1/m$ with half occupancy. Acceptable R and R_w values (0.035 and 0.040, respectively) were obtained, and the structure was chemically reasonable. A later examination of a second, solvated crystal, prompted by a reviewer's suggestion, gave a $\text{P}2_1/c$ cell, a and c axes corresponding to the 101 and 101 directions of the original refined cell. The true values of a and c were not identified by the autoindexing routine in the original cell refinement. Thus, in effect only half of the unique data for the true cell were collected.

Subsequent experiments showed that crystallization of concentrated solutions of II in *n*-heptane afforded crystals of a different habit. A suitable pseudohexagonal prism of dimensions 0.20 × 0.20 × 0.18 mm was selected for preliminary examination.

The crystal belonged to the monoclinic system, with systematic absences $0k0$, $k = 2n + 1$, and $h0l$, $h + l = 2n + 1$. Unit cell parameters refined from the least-squares refinement of 15 accurately centered reflections, are given in Table I. With $Z = 4$, the unit cell volume and measured density indicated the absence of solvent of crystallization. The structure of II reported in this paper is based on the intensity data collected for this unsolvated crystal. The data crystal was coated with epoxy resin to minimize loss of carbon monoxide, and intensities were measured as for I above using variable θ -2 θ scan speeds of 2.93 – $29.3^\circ \text{ min}^{-1}$. The two standard reflections 006 and 512 monitored over the course of data collected showed an intensity decrease of 12%; appropriate scaling of data was carried out. From 4952 independent measurements ($2\theta \leq 45^\circ$), 3425 had intensities $I \geq 3\sigma(I)$. These were considered observed and used in the solution and refinement.

Solution and Refinement of the Structures. $\text{Ru}_5(\text{CO})_{13}(\text{C}\equiv\text{CPh})(\text{PPh}_3)$. A Patterson synthesis readily yielded positions for all five ruthenium atoms. Standard Fourier methods allowed the location of all remaining non-hydrogen atoms. Refinement of positional and isotropic temperature factors gave an R value ($R = \sum|F_o| - |F_c|/\sum|F_o|$) of 0.07. With all non-hydrogen atoms assigned anisotropic thermal parameters, including the effects of anomalous dispersion for ruthenium, full-matrix least-squares refinement converged to $R = 0.033$. With a weighting scheme of the type $w^{-1} = 1.33 - 0.0088|F_o| + 0.00006|F_o|^2$ the weighted R factor ($R_w = [\sum w|F_o| - |F_c|^2]/\sum w|F_o|^2$) was 0.039. A final three-dimensional difference Fourier map showed no unusual features. The highest electron density ($0.5 \text{ e}/\text{\AA}^3$) was located in the region of Ru(4).

$\text{Ru}_5(\text{CO})_{14}(\text{C}\equiv\text{CPh})(\text{PPh}_2)$. An initial Patterson map yielded positions for all five ruthenium atoms. A Fourier synthesis phased with the heavy atoms clearly indicated locations for the phosphorus atom and the majority of the light atoms. Refinement of positions and isotropic temperature factors for all atoms gave an R value of 0.062. Conversion to anisotropic coefficients, followed by two cycles of least-squares refinement using the full matrix, reduced R to 0.038. A difference Fourier map calculated at this stage gave reasonable positions for all hydrogen atoms. In subsequent calculations these were included and isotropic thermal parameters refined. Refinement to convergence gave $R = 0.033$ with R_w , the weighted residual, = 0.037 where the weighting scheme had the form $w^{-1} = 1.52 - 0.0085|F_o| + 0.00005|F_o|^2$. A final difference map was featureless with maximum electron density of $0.7 \text{ e}/\text{\AA}^3$. The refined structure is basically the same as that found for the heptane solvate. However, the refinement is more satisfying in that all atoms refined well with anisotropic coefficients (in the solvate one carbonyl group was refined isotropically), and the problems of solvent disorder were avoided.

All calculations, carried out on IBM 360-75 and 4341 systems in the University of Waterloo Computing Centre, employed the full matrix. Scattering factors were taken from the tabulations of ref 11 and programs used are those described elsewhere.^{12,13} Atomic positions for I and II are listed in Tables II and III. Thermal parameters are available as supplementary material (Tables S1 and S2), and lists of structure factors have been deposited.

^{13}CO Exchange Experiments. A solution of $\text{Ru}_5(\text{CO})_{13}(\mu_4\eta^2\text{-C}\equiv\text{CPh})(\mu\text{-PPh}_2)$ (0.1 g, 0.087 mmol) in THF (10 mL) was placed in a 25-mL reaction vessel which was then evacuated and frozen in liquid nitrogen. During warming ^{13}CO was introduced to a pressure of ~ 2 atm and the mixture stirred at 25°C for 8 h. After this time the atmosphere was pumped away and the process repeated. Comparison of the intensities of the $\nu(\text{CO})$ bands (vide supra) with those of the exchanged compound ($\nu(^{13}\text{CO})$ (C_6H_{12}) 2021 (m), 1997 (vs), 1979 (s), 1968 (m), 1942 (w, sh) cm^{-1}) indicated that the level of ^{13}CO enrichment was $\sim 90\%$.

A ^{13}CO exchanged sample of II was obtained by bubbling ^{13}CO through the exchanged sample of I (~ 50 mg) in an NMR tube

Table II. Atomic Positions (Fractional $\times 10^4$) for $\text{Ru}_5(\text{CO})_{13}(\mu_4\eta^2\text{-C}\equiv\text{CPh})(\mu\text{-PPh}_2)$

atom	<i>x</i>	<i>y</i>	<i>z</i>
Ru(1)	-421.1 (7)	-412.1 (4)	1809.5 (3)
Ru(2)	918.7 (7)	1024.6 (4)	1657.2 (3)
Ru(3)	1871.8 (7)	59.3 (4)	2703.9 (3)
Ru(4)	-815.6 (7)	122.0 (4)	3021.1 (3)
Ru(5)	400.3 (7)	1512.3 (4)	2852.1 (3)
P	-214 (2)	1093 (1)	3759 (1)
O(1)	948 (8)	-1096 (4)	786 (3)
O(2)	-3294 (8)	-966 (5)	1205 (4)
O(3)	-89 (9)	-1942 (4)	2562 (3)
O(4)	1505 (10)	698 (5)	349 (4)
O(5)	3899 (8)	1461 (5)	2156 (4)
O(6)	326 (9)	2759 (4)	1352 (4)
O(7)	4066 (7)	821 (5)	3677 (4)
O(8)	3771 (8)	-801 (5)	1955 (4)
O(9)	2124 (8)	-1273 (5)	3638 (4)
O(10)	-3884 (7)	86 (5)	2864 (4)
O(11)	-821 (8)	-1312 (4)	3854 (3)
O(12)	-1377 (8)	2959 (4)	2564 (4)
O(13)	2790 (7)	2583 (4)	3354 (4)
C(1)	437 (10)	-823 (6)	1165 (4)
C(2)	-2236 (11)	-756 (6)	1429 (5)
C(3)	-155 (11)	-1345 (6)	2322 (4)
C(4)	1279 (12)	798 (6)	830 (5)
C(5)	2796 (11)	1233 (6)	2005 (5)
C(6)	565 (10)	2109 (7)	1483 (5)
C(7)	3214 (10)	580 (6)	3302 (5)
C(8)	3054 (9)	-465 (6)	2218 (4)
C(9)	1941 (10)	-763 (6)	3280 (5)
C(10)	-2742 (9)	97 (5)	2919 (4)
C(11)	-797 (9)	-767 (5)	3547 (4)
C(12)	-678 (9)	2427 (6)	2681 (4)
C(13)	1899 (9)	2169 (6)	3169 (4)
C(14)	-748 (8)	760 (5)	2189 (4)
C(15)	-1242 (9)	792 (4)	1572 (4)
C(16)	-2452 (8)	1040 (5)	1124 (4)
C(17)	-3484 (10)	1444 (7)	1326 (4)
C(18)	-4631 (12)	1641 (8)	893 (5)
C(19)	-4754 (11)	1436 (7)	281 (5)
C(20)	-3724 (12)	1054 (7)	76 (4)
C(21)	-2566 (11)	859 (6)	492 (4)
C(22)	-1557 (8)	1614 (5)	4078 (4)
C(23)	-1461 (8)	1737 (5)	4716 (4)
C(24)	-2536 (11)	2094 (6)	4926 (4)
C(25)	-3701 (10)	2321 (6)	4521 (5)
C(26)	-3771 (9)	2196 (5)	3905 (4)
C(27)	-2724 (9)	1848 (4)	3677 (4)
C(28)	1170 (9)	998 (5)	4436 (4)
C(29)	1642 (10)	268 (5)	4676 (4)
C(30)	2775 (11)	229 (7)	5146 (5)
C(31)	3454 (10)	918 (8)	5368 (5)
C(32)	2988 (11)	1636 (7)	5133 (5)
C(33)	1856 (10)	1686 (6)	4665 (5)

until the color changed from dark green to brown (~ 30 s). Gas bubbling was continued for a further 30 s, the tube was rapidly sealed, and the ^{13}C NMR spectrum was recorded immediately. Samples of I and II prepared as above were shown to be uniformly exchanged at all sites by comparison of ^{13}C NMR spectra of nonenriched compounds.

Results and Discussion

Synthesis and Structural Characterization of I. Fragmentation of the monosubstituted ruthenium carbonyl derivatives $\text{Ru}_3(\text{CO})_{11}(\text{Ph}_2\text{PC}\equiv\text{CR})$ ($\text{R} = \text{Ph}, t\text{-Bu}, i\text{-Pr}$) under thermal, chemical (Me_3NO), or photochemical activation provides a useful route to a variety of phosphido-bridged ruthenium clusters with $\mu\text{-}\eta$ -bound acetylides.¹⁴ The success of these reactions for cluster synthesis relies on the facile cleavage of P–C(sp) bonds of phosphorus-coordinated phosphinoalkynes in the presence of a metal carbonyl fragment capable of intra- or intermolecular in-

(11) "International Tables for X-ray Crystallography"; Kynoch Press: Birmingham, 1975; Vol. IV.

(12) Carty, A. J.; Mott, G. N.; Taylor, N. J.; Yule, J. E. *J. Am. Chem. Soc.* 1978, 100, 3051.

(13) Touchard, D.; LeBozec, H.; Dixneuf, P. H.; Carty, A. J.; Taylor, N. J. *Inorg. Chem.* 1981, 20, 1811.

(14) Carty, A. J. *Pure Appl. Chem.* 1982, 54, 113.

Table III. Atomic Positions (Fractional $\times 10^4$) for $\text{Ru}_5(\text{CO})_{13}(\mu_4\text{-}\eta^2\text{-C}\equiv\text{CPh})(\mu\text{-PPh}_2)$

atom	x	y	z
Ru(1)	-1251.5 (4)	75.8 (6)	2856.2 (4)
Ru(2)	898.4 (4)	602.5 (6)	2409.8 (4)
Ru(3)	518.0 (4)	-513.5 (6)	3494.9 (4)
Ru(4)	-809.4 (4)	-1819.0 (5)	2374.8 (4)
Ru(5)	803.7 (4)	-1728.6 (5)	2413.4 (4)
P	89 (1)	-3260 (2)	2558 (1)
O(1)	-1407 (5)	2528 (6)	3027 (6)
O(2)	-3078 (4)	-190 (6)	1798 (4)
O(3)	-1553 (5)	-387 (8)	4278 (5)
O(4)	2587 (5)	1679 (8)	3427 (5)
O(5)	-72 (6)	2686 (6)	2469 (5)
O(6)	556 (5)	1303 (7)	801 (5)
O(7)	2405 (4)	-824 (7)	4380 (4)
O(8)	575 (5)	1692 (6)	4262 (4)
O(9)	217 (5)	-1857 (6)	4674 (4)
O(10)	-2277 (5)	-2574 (6)	950 (4)
O(11)	-1593 (5)	-2770 (6)	3343 (5)
O(12)	455 (5)	-2442 (6)	801 (4)
O(13)	2402 (4)	-3024 (6)	3260 (4)
O(14)	2293 (4)	-711 (6)	2267 (4)
C(1)	-1327 (6)	1619 (8)	2982 (6)
C(2)	-2397 (5)	-57 (7)	2209 (5)
C(3)	-1409 (6)	-224 (8)	3771 (6)
C(4)	1955 (6)	1315 (9)	3049 (6)
C(5)	264 (6)	1907 (8)	2447 (6)
C(6)	696 (6)	1035 (9)	1402 (6)
C(7)	1709 (6)	-732 (8)	4205 (5)
C(8)	497 (6)	877 (8)	3955 (5)
C(9)	296 (6)	-1389 (8)	4214 (5)
C(10)	-1709 (6)	-2316 (8)	1478 (6)
C(11)	-1312 (6)	-2381 (8)	2977 (6)
C(12)	587 (6)	-2187 (7)	1410 (6)
C(13)	1802 (6)	-2548 (7)	2956 (5)
C(14)	1680 (5)	-640 (8)	2342 (5)
C(15)	-137 (5)	-319 (6)	2283 (4)
C(16)	-987 (5)	-61 (6)	1931 (4)
C(17)	-1429 (5)	317 (7)	1139 (4)
C(18)	-1359 (6)	-204 (9)	532 (5)
C(19)	-1763 (7)	213 (11)	-215 (6)
C(20)	-2232 (7)	1154 (10)	-345 (6)
C(21)	-2308 (7)	1687 (9)	227 (6)
C(22)	-1923 (6)	1274 (7)	972 (5)
C(23)	-57 (6)	-4360 (7)	1860 (5)
C(24)	620 (7)	-4937 (8)	1918 (7)
C(25)	570 (10)	-5713 (10)	1398 (8)
C(26)	-159 (12)	-5933 (11)	817 (7)
C(27)	-863 (13)	-5419 (14)	758 (9)
C(28)	-800 (10)	-4599 (11)	1291 (8)
C(29)	465 (5)	-4049 (6)	3440 (5)
C(30)	1125 (5)	-3731 (7)	4127 (5)
C(31)	1300 (6)	-4324 (9)	4782 (5)
C(32)	850 (6)	-5237 (8)	4778 (5)
C(33)	208 (6)	-5578 (8)	4101 (6)
C(34)	18 (5)	-4977 (8)	3430 (5)

teraction with the alkyne triple bond. Thus $\text{Fe}(\text{CO})_4\text{-}(\text{Ph}_2\text{PC}\equiv\text{C}-t\text{-Bu})$ reacts smoothly with $[\text{Fe}(\text{CO})_4]$ generated from $\text{Fe}_2(\text{CO})_9$ to give an intermediate $(\text{CO})_4\text{Fe}\{\text{PPh}_2\text{C}\equiv\text{C}-t\text{-Bu}\}\text{Fe}(\text{CO})_4$ derivative¹⁵ which smoothly undergoes P-C cleavage on warming with CO dissociation and Fe-Fe bond formation giving $\text{Fe}_2(\text{CO})_6(\mu\text{-PPh}_2)(\mu_4\text{-}\eta^2\text{-C}\equiv\text{C}-t\text{-Bu})$.¹⁶ In the precursor $\text{Ru}_3(\text{CO})_{11}(\text{Ph}_2\text{PC}\equiv\text{CPh})$ the phosphorus atom of the phosphinoalkyne occupies an equatorial site on one ruthenium atom, with a pendant $\text{C}\equiv\text{CPh}$ unit available for interaction either with an adjacent ruthenium atom or with a second cluster unit.^{7b} Since higher ruthenium clusters are often sensitive to thermal degradation, conditions for their synthesis must

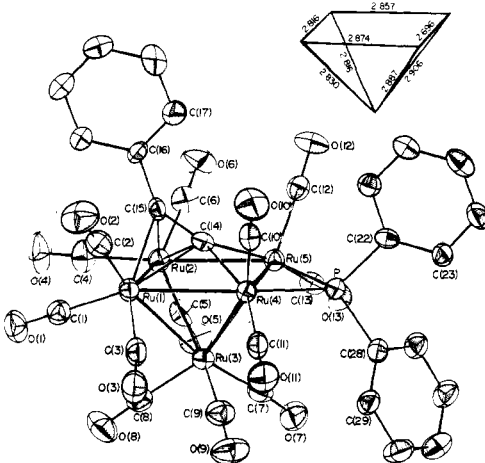


Figure 1.

be sufficiently mild to prevent cluster fragmentation while allowing the sequestering of ruthenium units by ligand fragments generated in situ. In the present case the pentanuclear cluster $\text{Ru}_5(\text{CO})_{13}(\mu_4\text{-}\eta^2\text{-C}\equiv\text{CPh})(\text{PPh}_2)$ is accessible in modest but workable yields from the thermolysis of $\text{Ru}_3(\text{CO})_{11}(\text{Ph}_2\text{PC}\equiv\text{CPh})$ in refluxing *n*-heptane (bp 98 °C). The blue-black compound is air stable in the solid state and sparingly soluble in saturated hydrocarbons and decomposes only slowly in degassed solvents over periods of several days.

An ORTEP II plot of the molecular structure of I is shown in Figure 1, with the metal skeleton and associated bond lengths inset. The cluster is one of relatively few pentanuclear ruthenium carbonyls. The only other examples of square-pyramidal Ru_5 compounds known to us are $\text{Ru}_5(\text{CO})_{15}(\mu_4\text{-PR})$ ($\text{R} = \text{Ph}, \text{Et}$),¹⁷ $\text{Ru}_5(\text{CO})_{13}(\mu_3\text{-}\eta^2\text{-PhC}\equiv\text{CPh})(\mu_4\text{-PPh})$,¹⁸ the carbido clusters $\text{Ru}_5(\text{CO})_{15}(\text{C})$ and $\text{Ru}_5(\text{CO})_{14}(\text{C})\text{PPh}_3$,^{9,19} and the vinylidene $\text{H}_2\text{Ru}_5(\text{CO})_{15}(\mu_4\text{-C}\equiv\text{CH}_2)$.²⁰ The skeleton of I is composed of eight strong metal-metal bonds, seven of which (Ru(1)-Ru(2) = 2.8165 (9) Å, Ru(1)-Ru(3) = 2.8294 (9) Å, Ru(1)-Ru(4) = 2.8742 (9) Å, Ru(2)-Ru(3) = 2.8163 (9) Å, Ru(2)-Ru(5) = 2.8567 (9) Å, Ru(3)-Ru(4) = 2.8863 (9) Å, Ru(3)-Ru(5) = 2.9052 (9) Å) are in the normal range²¹ for ruthenium-ruthenium bonds in clusters. The Ru(4)-Ru(5) distance along the remaining edge of the cluster bridged by the phosphido group is significantly shorter (2.6965 (9) Å), a feature which may be pertinent to the structural changes which accompany adduct formation (vide infra). The basal plane of the pyramid is defined by atoms Ru(1), Ru(2), Ru(4), and Ru(5). The maximum atomic displacement of any basal metal from this plane is 0.02 Å, which compares with a similar value of 0.16 Å in the related cluster $\text{Ru}_5(\text{CO})_{15}(\mu_4\text{-PPh})$.¹⁷ The apical atom Ru(3) lies 2.086 Å below the best plane through Ru(1), Ru(2), Ru(4), and Ru(5) but

(17) Natarajan, K.; Zsolnai, L.; Huttner, G. *J. Organomet. Chem.* 1981, 209, 85.

(18) MacLaughlin, S. A.; Taylor, N. J.; Carty, A. J. to be submitted for publication. See also ref 14, p 129, for an ORTEP plot.

(19) (a) Farrar, D. H.; Jackson, P. F.; Johnson, B. F. G.; Lewis, J.; Nicholls, J. N.; McPartlin, M. *J. Chem. Soc. Chem. Commun.* 1981, 415. (b) Johnson, B. F. G.; Lewis, J.; Nicholls, J. N.; Ruga, J.; Raithby, P. R.; Rosales, M. J.; McPartlin, M.; Clegg, W. *J. Chem. Soc., Dalton Trans.* 1982, 277.

(20) Eady, C. R.; Johnson, B. F. G.; Lewis, J. *J. Chem. Soc., Dalton Trans.* 1977, 477.

(21) Churchill, M. R.; Hollander, F. J.; Hutchinson, J. P. *Inorg. Chem.* 1977, 16, 2655.

(22) Carty, A. J.; Taylor, N. J.; Smith, W. F. *J. Chem. Soc., Chem. Commun.* 1979, 750.

(23) Catti, M.; Gervasio, G.; Mason, S. A. *J. Chem. Soc., Dalton Trans.* 1977, 2260.

(15) Carty, A. J.; Smith, W. F.; Taylor, N. J. *J. Organomet. Chem.* 1978, 146, C1.

(16) Smith, W. F.; Yule, J. E.; Taylor, N. J.; Paik, H. N.; Carty, A. J. *Inorg. Chem.* 1977, 16, 1593.

Table IV. A Selection of Bond Lengths (Å) and Angles (deg) for $\text{Ru}_5(\text{CO})_{13}(\mu_4\text{-}\eta^2\text{-C}\equiv\text{CPh})(\mu\text{-PPh}_2)$

A. Bond Lengths				
$\text{Ru}(1)\text{-Ru}(2)$	2.8165 (9)	$\text{Ru}(5)\text{-C}(14)$	2.095 (8)	$\text{C}(14)\text{-C}(15)$
$\text{Ru}(1)\text{-Ru}(3)$	2.8294 (9)	$\text{Ru}(1)\text{-C}(1)$	1.899 (9)	$\text{C}(15)\text{-C}(16)$
$\text{Ru}(1)\text{-Ru}(4)$	2.8742 (9)	$\text{Ru}(1)\text{-C}(2)$	1.935 (11)	$\text{C}(1)\text{-O}(1)$
$\text{Ru}(2)\text{-Ru}(3)$	2.8163 (9)	$\text{Ru}(1)\text{-C}(3)$	1.918 (10)	$\text{C}(3)\text{-O}(3)$
$\text{Ru}(2)\text{-Ru}(5)$	2.8567 (9)	$\text{Ru}(2)\text{-C}(4)$	1.932 (11)	$\text{C}(4)\text{-O}(4)$
$\text{Ru}(3)\text{-Ru}(4)$	2.8863 (9)	$\text{Ru}(2)\text{-C}(5)$	1.918 (11)	$\text{C}(5)\text{-O}(5)$
$\text{Ru}(3)\text{-Ru}(5)$	2.9052 (9)	$\text{Ru}(2)\text{-C}(6)$	1.888 (11)	$\text{C}(6)\text{-O}(6)$
$\text{Ru}(4)\text{-Ru}(5)$	2.6965 (9)	$\text{Ru}(3)\text{-C}(7)$	1.900 (10)	$\text{C}(7)\text{-O}(7)$
$\text{Ru}(4)\text{-P}$	2.294 (2)	$\text{Ru}(3)\text{-C}(8)$	1.933 (10)	$\text{C}(8)\text{-O}(8)$
$\text{Ru}(5)\text{-P}$	2.278 (2)	$\text{Ru}(3)\text{-C}(9)$	1.861 (11)	$\text{C}(9)\text{-O}(9)$
$\text{Ru}(1)\text{-C}(14)$	2.190 (8)	$\text{Ru}(4)\text{-C}(10)$	1.893 (9)	$\text{C}(10)\text{-O}(10)$
$\text{Ru}(1)\text{-C}(15)$	2.216 (8)	$\text{Ru}(4)\text{-C}(11)$	1.884 (9)	$\text{C}(11)\text{-O}(11)$
$\text{Ru}(2)\text{-C}(15)$	2.163 (9)	$\text{Ru}(5)\text{-C}(12)$	1.879 (9)	$\text{C}(12)\text{-O}(12)$
$\text{Ru}(4)\text{-C}(14)$	2.114 (8)	$\text{Ru}(5)\text{-C}(13)$	1.886 (9)	$\text{C}(13)\text{-O}(13)$
B. Bond Angles				
(i) M-M-M				
$\text{Ru}(2)\text{-Ru}(1)\text{-Ru}(3)$	59.8 (0)	$\text{Ru}(1)\text{-Ru}(4)\text{-Ru}(3)$	58.8 (0)	$\text{Ru}(2)\text{-Ru}(3)\text{-Ru}(4)$
$\text{Ru}(2)\text{-Ru}(1)\text{-Ru}(4)$	89.1 (1)	$\text{Ru}(1)\text{-Ru}(4)\text{-Ru}(5)$	90.5 (0)	$\text{Ru}(2)\text{-Ru}(3)\text{-Ru}(5)$
$\text{Ru}(3)\text{-Ru}(1)\text{-Ru}(4)$	60.8 (0)	$\text{Ru}(3)\text{-Ru}(4)\text{-Ru}(5)$	62.6 (0)	$\text{Ru}(4)\text{-Ru}(3)\text{-Ru}(5)$
$\text{Ru}(1)\text{-Ru}(2)\text{-Ru}(3)$	60.3 (0)	$\text{Ru}(1)\text{-Ru}(3)\text{-Ru}(2)$	59.9 (0)	$\text{Ru}(2)\text{-Ru}(5)\text{-Ru}(3)$
$\text{Ru}(1)\text{-Ru}(2)\text{-Ru}(5)$	88.5 (0)	$\text{Ru}(1)\text{-Ru}(3)\text{-Ru}(4)$	60.4 (1)	$\text{Ru}(2)\text{-Ru}(5)\text{-Ru}(4)$
$\text{Ru}(3)\text{-Ru}(2)\text{-Ru}(5)$	61.6 (0)	$\text{Ru}(1)\text{-Ru}(3)\text{-Ru}(5)$	87.3 (0)	$\text{Ru}(3)\text{-Ru}(5)\text{-Ru}(4)$
(ii) M-M-P				
$\text{Ru}(1)\text{-Ru}(4)\text{-P}$	143.2 (9)	$\text{Ru}(2)\text{-Ru}(5)\text{-P}$	144.7 (0)	$\text{Ru}(4)\text{-Ru}(5)\text{-P}$
$\text{Ru}(3)\text{-Ru}(4)\text{-P}$	98.3 (0)	$\text{Ru}(3)\text{-Ru}(5)\text{-P}$	93.1 (0)	$\text{Ru}(5)\text{-Ru}(4)\text{-P}$
(iii) M-P-M, M-P-C, C-P-C				
$\text{Ru}(4)\text{-P-Ru}(5)$	72.3 (0)	$\text{Ru}(4)\text{-P-C}(28)$	124.1 (2)	$\text{Ru}(5)\text{-P-C}(28)$
$\text{Ru}(4)\text{-P-C}(22)$	119.3 (2)	$\text{Ru}(5)\text{-O-C}(22)$	120.4 (2)	$\text{C}(22)\text{-P-C}(28)$
(iv) M-M-C				
$\text{Ru}(1)\text{-Ru}(2)\text{-C}(14)$	49.8 (2)	$\text{Ru}(3)\text{-Ru}(1)\text{-C}(3)$	79.9 (3)	$\text{Ru}(4)\text{-Ru}(3)\text{-C}(8)$
$\text{Ru}(1)\text{-Ru}(2)\text{-C}(15)$	50.8 (2)	$\text{Ru}(4)\text{-Ru}(1)\text{-C}(1)$	160.7 (2)	$\text{Ru}(4)\text{-Ru}(3)\text{-C}(9)$
$\text{Ru}(2)\text{-Ru}(1)\text{-C}(14)$	51.1 (2)	$\text{Ru}(4)\text{-Ru}(1)\text{-C}(2)$	102.2 (3)	$\text{Ru}(5)\text{-Ru}(3)\text{-C}(7)$
$\text{Ru}(2)\text{-Ru}(1)\text{-C}(15)$	49.1 (2)	$\text{Ru}(4)\text{-Ru}(1)\text{-C}(3)$	75.8 (3)	$\text{Ru}(5)\text{-Ru}(3)\text{-C}(8)$
$\text{Ru}(2)\text{-Ru}(5)\text{-C}(14)$	50.8 (2)	$\text{Ru}(1)\text{-Ru}(2)\text{-C}(4)$	96.4 (3)	$\text{Ru}(5)\text{-Ru}(3)\text{-C}(9)$
$\text{Ru}(3)\text{-Ru}(1)\text{-C}(14)$	69.2 (2)	$\text{Ru}(1)\text{-Ru}(2)\text{-C}(5)$	124.1 (3)	$\text{Ru}(1)\text{-Ru}(4)\text{-C}(14)$
$\text{Ru}(3)\text{-Ru}(1)\text{-C}(15)$	96.9 (2)	$\text{Ru}(1)\text{-Ru}(2)\text{-C}(6)$	141.5 (3)	$\text{Ru}(3)\text{-Ru}(4)\text{-C}(14)$
$\text{Ru}(3)\text{-Ru}(2)\text{-C}(14)$	68.9 (2)	$\text{Ru}(3)\text{-Ru}(2)\text{-C}(4)$	122.8 (3)	$\text{Ru}(5)\text{-Ru}(4)\text{-C}(14)$
$\text{Ru}(3)\text{-Ru}(2)\text{-C}(15)$	98.5 (2)	$\text{Ru}(3)\text{-Ru}(2)\text{-C}(5)$	68.1 (3)	$\text{Ru}(1)\text{-Ru}(4)\text{-C}(10)$
$\text{Ru}(3)\text{-Ru}(5)\text{-C}(14)$	68.7 (2)	$\text{Ru}(3)\text{-Ru}(2)\text{-C}(6)$	138.2 (3)	$\text{Ru}(1)\text{-Ru}(4)\text{-C}(11)$
$\text{Ru}(4)\text{-Ru}(1)\text{-C}(14)$	47.0 (2)	$\text{Ru}(5)\text{-Ru}(2)\text{-C}(4)$	174.7 (3)	$\text{Ru}(3)\text{-Ru}(4)\text{-C}(10)$
$\text{Ru}(4)\text{-Ru}(1)\text{-C}(15)$	76.6 (2)	$\text{Ru}(5)\text{-Ru}(2)\text{-C}(5)$	85.1 (3)	$\text{Ru}(3)\text{-Ru}(4)\text{-C}(11)$
$\text{Ru}(4)\text{-Ru}(5)\text{-C}(14)$	50.5 (2)	$\text{Ru}(5)\text{-Ru}(2)\text{-C}(6)$	81.1 (3)	$\text{Ru}(5)\text{-Ru}(4)\text{-C}(10)$
$\text{Ru}(5)\text{-Ru}(2)\text{-C}(14)$	46.7 (2)	$\text{Ru}(1)\text{-Ru}(3)\text{-C}(7)$	168.0 (2)	$\text{Ru}(5)\text{-Ru}(4)\text{-C}(11)$
$\text{Ru}(5)\text{-Ru}(2)\text{-C}(15)$	77.8 (2)	$\text{Ru}(1)\text{-Ru}(3)\text{-C}(8)$	89.6 (2)	$\text{Ru}(2)\text{-Ru}(5)\text{-C}(12)$
$\text{Ru}(2)\text{-Ru}(1)\text{-C}(1)$	86.6 (2)	$\text{Ru}(1)\text{-Ru}(3)\text{-C}(9)$	100.2 (3)	$\text{Ru}(2)\text{-Ru}(5)\text{-C}(13)$
$\text{Ru}(2)\text{-Ru}(1)\text{-C}(2)$	129.4 (3)	$\text{Ru}(2)\text{-Ru}(3)\text{-C}(7)$	112.1 (2)	$\text{Ru}(3)\text{-Ru}(5)\text{-C}(12)$
$\text{Ru}(2)\text{-Ru}(1)\text{-C}(3)$	139.2 (3)	$\text{Ru}(2)\text{-Ru}(3)\text{-C}(8)$	88.5 (2)	$\text{Ru}(3)\text{-Ru}(5)\text{-C}(13)$
$\text{Ru}(3)\text{-Ru}(1)\text{-C}(1)$	101.1 (2)	$\text{Ru}(2)\text{-Ru}(3)\text{-C}(9)$	159.9 (3)	$\text{Ru}(4)\text{-Ru}(5)\text{-C}(12)$
$\text{Ru}(3)\text{-Ru}(1)\text{-C}(2)$	162.2 (3)	$\text{Ru}(4)\text{-Ru}(3)\text{-C}(7)$	112.8 (2)	$\text{Ru}(4)\text{-Ru}(5)\text{-C}(13)$
(v) M-C-M, M-C-C, C-C-C				
$\text{Ru}(1)\text{-C}(14)\text{-Ru}(2)$	79.1 (0)	$\text{Ru}(2)\text{-C}(14)\text{-Ru}(5)$	82.5 (0)	$\text{Ru}(1)\text{-C}(15)\text{-Ru}(2)$
$\text{Ru}(1)\text{-C}(14)\text{-Ru}(4)$	83.8 (0)	$\text{Ru}(2)\text{-C}(14)\text{-C}(15)$	69.4 (3)	$\text{Ru}(1)\text{-C}(15)\text{-C}(14)$
$\text{Ru}(1)\text{-C}(14)\text{-Ru}(5)$	134.9 (0)	$\text{Ru}(4)\text{-C}(14)\text{-Ru}(5)$	79.7 (0)	$\text{Ru}(2)\text{-C}(15)\text{-C}(14)$
$\text{Ru}(1)\text{-C}(14)\text{-C}(15)$	73.3 (3)	$\text{Ru}(4)\text{-C}(14)\text{-C}(15)$	144.1 (3)	$\text{Ru}(2)\text{-C}(15)\text{-C}(16)$
$\text{Ru}(2)\text{-C}(14)\text{-Ru}(4)$	183.3 (0)	$\text{Ru}(5)\text{-C}(14)\text{-C}(15)$	135.8 (3)	$\text{C}(14)\text{-C}(15)\text{-C}(16)$

is asymmetrically located with respect to the $\text{Ru}(1)\text{-Ru}(2)$ (average $\text{Ru}(3)\text{-Ru} = 2.823 \text{ \AA}$) and $\text{Ru}(4)\text{-Ru}(5)$ (average $\text{Ru}(3)\text{-Ru} = 2.896 \text{ \AA}$) vectors.

Apart from the metal framework the principal structural feature of interest is the multisite-bound acetylide which is $\mu_4\text{-}\eta^2$ coordinated to the upper, square face of the cluster. The α -carbon atom C(14) symmetrically bridges the $\text{Ru}(4)\text{-Ru}(5)$ edge with the triply bonded atoms C(14) and C(15) engaged in perpendicular η^2 interactions with $\text{Ru}(1)$ and $\text{Ru}(2)$. Although there are statistically significant differences between individual $\text{Ru}(1)$ - and $\text{Ru}(2)$ -acetylidyde distances ($\text{Ru}(1)\text{-C}(14) = 2.190$ (8) \AA , $\text{Ru}(2)\text{-C}(14) = 2.234$ (8) \AA , $\text{Ru}(1)\text{-C}(15) = 2.216$ (8) \AA , $\text{Ru}(2)\text{-C}(15) = 2.163$ (9) \AA), the overall η^2 bonding is fairly symmetrical. The α -carbon atom C(14) is however more strongly bonded to

$\text{Ru}(4)$ and $\text{Ru}(5)$ (average $\text{Ru-C}(14) = 2.105 \text{ \AA}$) than to $\text{Ru}(1)$ and $\text{Ru}(2)$ (average $\text{Ru-C}(14) = 2.212 \text{ \AA}$) resulting in a slight displacement of this atom towards the $\text{Ru}(4)\text{-Ru}(5)$ edge.

Of major interest to cluster chemists are the structural modifications and ligand reactivity which accompany multisite binding on a cluster surface. Characterization of I as a μ_4 -acetylidyde affords an opportunity to examine the effect of successively increasing the number of metal atoms interacting with a single acetylidyde since examples of μ , $\mu\text{-}\eta^2$, and $\mu_3\text{-}\eta^2$ bonding to the same metal, ruthenium, are now known. Pertinent comparisons are illustrated in Table VI. In general an increase in the number of interacting metals increases the C-C acetylidyde bond length, decreases the Ru-C distances to the η -bound carbond

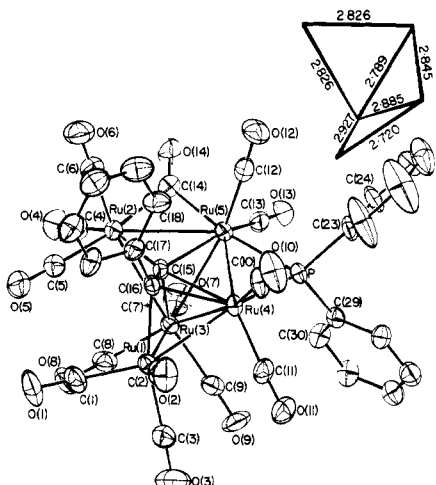


Figure 2.

atoms, and increases the distortion of the acetylide from linearity. The rather long C(14)-C(15) distance (1.342 (11) Å) in I, a value characteristic of carbon-carbon double bonds in olefins, is notable.

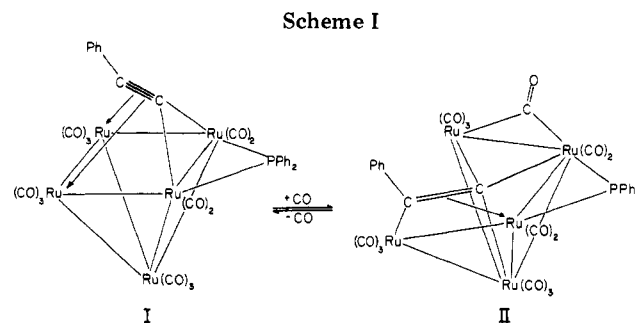
Replacement of the three-electron donor phosphido bridge and the five-electron donor acetylide in I by two carbonyl groups and a carbide ligand would give the iso-electronic molecule $\text{Ru}_5(\text{CO})_{15}(\text{C})$ which has recently been structurally characterized.¹⁹ There are rather striking structural similarities between I and the carbido cluster $\text{Ru}_5(\text{CO})_{15}(\text{C})$. Both have square-pyramidal metal frameworks, and the carbido atom in $\text{Ru}_5(\text{CO})_{15}(\text{C})$ lies 0.11 Å above the basal plane compared to 0.06 Å for C(14) in I. There are indications that the chemistry of the carbido cluster^{9,19} may show some similarities to that of I.

Synthesis and Structural Characterization of II.

In the course of the preparation of ^{13}CO exchanged samples for ^{13}C NMR experiments, it was observed that under 2 atm of ^{13}CO the relatively insoluble blue green (I) rapidly dissolved in heptane to give an orange/brown solution. An X-ray crystallographic analysis of the product revealed it to be the CO adduct $\text{Ru}_5(\text{CO})_{13}(\mu\text{-CO})(\mu_5\text{-}\eta^2\text{-C}\equiv\text{CPh})(\mu\text{-PPPh}_2)$. An ORTEP II diagram of this extraordinary cluster is given in Figure 2 along with bond length data for the metal skeleton (inset). The pentanuclear framework consists of three Ru_3 triangles with the central triangle sharing two edges. Alternatively the structure can be described as a double butterfly or "swallowlike" structure. This stereochemical array is highly unusual for metal clusters, the only other example being the recently reported $\text{Ru}_5(\text{CO})_{14}(\text{CN-}t\text{-Bu})_2$.²⁴

With the assumption, as seems reasonable in view of the mild conditions employed in the synthesis and the reversibility of the conversion of I to II, that the phosphido bridge of I remains intact, formation of II involves opening of the square pyramid of I along the basal edge opposite to that bridged by the PPh_2 group. Both the metal framework and the acetylide undergo dramatic rearrangement during this process (Scheme I).

Within the Ru₅ skeleton, six of the intermetallic distances are within the normal range of 2.70–2.90 Å for Ru–Ru bonds^{14,21,25} (Ru(1)–Ru(4) = 2.720 (1) Å, Ru(2)–Ru(3) = 2.826 (1) Å, Ru(2)–Ru(5) = 2.826 (1) Å, Ru(3)–Ru(4) = 2.885 (1) Å, Ru(3)–Ru(5) = 2.789 (1) Å, Ru(4)–Ru(5) = 2.845 (1) Å) while the Ru(1)–Ru(3) bond length



Scheme I

(2.927 (1) Å) is slightly longer. The Ru(1)…Ru(2) distance of 4.330 Å precludes any bonding interaction between these atoms. Comparison of bond lengths for I and II shows that adduct formation results in Ru(1)…Ru(2) bond cleavage, lengthening of the phosphido-bridged edge Ru(4)–Ru(5), and the Ru(1)–Ru(3) edge, and shortening of the Ru(3)–Ru(5) bond.

Figures 1 and 2 quite clearly show that the carbonyl substitution pattern in II is the same as that in the precursor I. Thus the apical atom Ru(3) in I also has three carbonyl groups in II, the PPh_3 -bridged atoms (Ru(4) and Ru(5) carry two CO groups each, and the acetylidy bridged atoms Ru(1) and Ru(2) retain three terminal carbonyls. The additional CO group is located as a symmetrical μ -bridge across the Ru(2)-Ru(5) edge. In contrast, $\text{Ru}_5(\text{CO})_{14}(\text{CN}-t\text{-Bu})_2$ ²⁴ has a semibridging CO across one hinge edge.

Examination of the ORTEP drawings of I and II shows that the "opening" of the square pyramid of I via addition of a two-electron donor presents a cavity into which the α -carbon atom of the phenyl acetylidyne "sinks" (Figure 2). Thus the α -carbon atom becomes partially encapsulated by the cluster with bonding interactions to four metal atoms (Ru(2)–Ru(5)). Whereas the acetylidyne in I interacted with only the basal atoms of the square pyramid, in II all five metal atoms are involved in bonding. A modified description of this multisite interaction is therefore necessary. Examination of Figure 2 and Table V shows that C(15) is strongly bonded in fairly symmetrical fashion to Ru(2) (Ru(2)–C(15) = 2.076 (9) Å) and Ru(3) (Ru(3)–C(15) = 2.135 (8) Å), with a weaker interaction to Ru(5) (Ru(5)–C(15) = 2.326 (9) Å). The α -carbon atom C(15) thus caps the inner Ru(2)–Ru(3)–Ru(5) face. The remaining acetylidyne–metal bonds are then an η^2 interaction of olefinic type with Ru(4) and a strong σ bond to Ru(1). As expected in view of the μ_5 -acetylidyne–cluster interaction the formal acetylenic bond C(15)–C(16) in II (1.39 (1) Å) is even longer than that in I (1.342 (9) Å) and the longest we have observed to date. The bend-back angle at C(16) (56.4 (4)°) is also extremely large; the C(15)–C(16)–C(17) angle (123.6 (4)°) is thus close to that expected for a free olefin.

The Phosphido Bridges in I and II. Figures 1 and 2 show that the phosphido bridges in cluster I and its CO adduct II occupy equatorial sites on ruthenium atoms Ru(4) and Ru(5). The phosphido bridge angles Ru(4)–P–Ru(5) (72.3 (0) and 76.0 (0)°, respectively) are acute and quite similar in the two molecules. However the phosphido-bridged metal–metal bond in I (2.6965 (9) Å) is much shorter than in II (2.845 (1) Å as are the Ru–P bond lengths (average Ru–P = 2.286 Å in I vs. 2.310 Å in II).

Cluster I has a very low-field chemical shift for the PPPh_2 group ($\delta^{31}\text{P} = +253$ ppm) which we would normally have attributed²⁶ to a small Ru-P-Ru angle and short Ru-Ru

(24) Bruce, M. I.; Matisons, J. G.; Rodgers, J. R.; Wallis, R. C. *J. Chem. Soc., Chem. Commun.* 1981, 1070.

(25) Carty, A. J.; MacLaughlin, S. A.; Van Wagner, J.; Taylor, N. J. *Organometallics* 1982, 1, 1013.

(26) (a) Carty, A. *J. Adv. Chem. Ser.* 1982, No. 196, 163. (b) Carty, A. J.; Hartstock, F.; Taylor, N. J. *Inorg. Chem.* 1982, 21, 1349.

Table V. A Selection of Bond Lengths (Å) and Bond Angles (deg) for $\text{Ru}_5(\text{CO})_{14}(\mu_5\text{-}\eta^2\text{-C}\equiv\text{CPh})(\mu\text{-PPh}_2)$

A. Bond Lengths					
Ru(1)-Ru(3)	2.927 (1)	P-C(23)	1.836 (9)	Ru(2)-C(6)	1.905 (11)
Ru(2)-Ru(3)	2.826 (1)	C(1)-O(1)	1.118 (13)	Ru(3)-C(8)	1.913 (10)
Ru(3)-Ru(4)	2.885 (1)	C(3)-O(3)	1.139 (14)	Ru(4)-C(10)	1.878 (10)
Ru(4)-Ru(5)	2.845 (1)	C(5)-O(5)	1.126 (14)	Ru(5)-C(12)	1.898 (10)
Ru(4)-P	2.287 (2)	C(7)-O(7)	1.130 (13)	Ru(2)-C(14)	2.093 (10)
Ru(1)-C(1)	1.895 (10)	C(9)-O(9)	1.120 (12)	Ru(3)-C(15)	2.135 (8)
Ru(1)-C(3)	1.952 (11)	C(11)-C(11)	1.136 (14)	Ru(5)-C(15)	2.326 (8)
Ru(2)-C(5)	1.962 (11)	C(13)-O(13)	1.126 (13)	Ru(4)-C(16)	2.265 (8)
Ru(3)-C(7)	1.929 (10)	C(15)-C(16)	1.398 (13)	P-C(29)	1.816 (8)
Ru(3)-C(9)	1.927 (10)	Ru(1)-Ru(4)	2.720 (1)	C(2)-O(2)	1.135 (13)
Ru(4)-C(11)	1.885 (11)	Ru(2)-Ru(5)	2.826 (1)	C(4)-O(4)	1.130 (15)
Ru(5)-C(13)	1.902 (10)	Ru(3)-Ru(5)	2.789 (1)	C(6)-O(6)	1.129 (14)
Ru(5)-C(14)	2.094 (10)	Ru(1)-·Ru(2)	4.330 (1)	C(8)-O(8)	1.130 (12)
Ru(2)-C(15)	2.076 (9)	Ru(5)-P	2.333 (2)	C(10)-O(10)	1.125 (13)
Ru(4)-C(15)	2.225 (8)	Ru(1)-C(2)	1.878 (10)	C(12)-O(12)	1.144 (12)
Ru(1)-C(16)	2.055 (8)	Ru(2)-C(4)	1.945 (12)	C(14)-O(14)	1.166 (13)
				C(16)-C(17)	1.463 (11)
B. Bond Angles					
(i) M-M-M					
Ru(3)-Ru(1)-Ru(4)	61.3 (0)	Ru(3)-Ru(4)-Ru(5)	58.3 (0)	Ru(4)-Ru(3)-Ru(5)	60.1 (0)
Ru(1)-Ru(3)-Ru(2)	97.6 (0)	Ru(2)-Ru(5)-Ru(4)	95.7 (0)	Ru(1)-Ru(4)-Ru(5)	113.6 (0)
Ru(1)-Ru(3)-Ru(5)	109.1 (0)	Ru(3)-Ru(2)-Ru(5)	59.1 (0)	Ru(2)-Ru(5)-Ru(3)	60.4 (0)
Ru(2)-Ru(3)-Ru(5)	60.4 (0)	Ru(1)-Ru(3)-Ru(4)	55.8 (0)	Ru(3)-Ru(5)-Ru(4)	61.6 (0)
Ru(1)-Ru(4)-Ru(3)	62.9 (0)	Ru(2)-Ru(3)-Ru(4)	94.8 (0)		
(ii) M-M-P					
Ru(1)-Ru(4)-P	151.3 (0)	Ru(3)-Ru(5)-P	92.2 (0)	Ru(2)-Ru(5)-P	146.0 (0)
Ru(5)-Ru(4)-P	52.7 (0)	Ru(3)-Ru(4)-P	90.7 (0)	Ru(4)-Ru(5)-P	51.3 (0)
(iii) M-P-M, M-P-C					
Ru(4)-P-Ru(5)	76.0 (0)	Ru(5)-P-C(29)	122.4 (2)	Ru(5)-P-C(23)	113.3 (2)
Ru(4)-P-C(29)	119.4 (2)	Ru(4)-P-C(23)	125.1 (2)	C(23)-P-C(29)	101.0 (3)
(iv) M-M-C					
Ru(3)-Ru(1)-C(1)	108.0 (3)	Ru(3)-Ru(4)-C(10)	163.9 (3)	Ru(1)-Ru(3)-C(8)	75.3 (3)
Ru(3)-Ru(1)-C(3)	97.2 (3)	Ru(3)-Ru(4)-C(15)	47.8 (2)	Ru(1)-Ru(3)-C(15)	62.5 (2)
Ru(4)-Ru(1)-C(1)	157.3 (3)	Ru(5)-Ru(4)-C(10)	118.6 (3)	Ru(2)-Ru(3)-C(8)	89.4 (3)
Ru(4)-Ru(1)-C(3)	109.6 (3)	Ru(5)-Ru(4)-C(15)	52.9 (2)	Ru(2)-Ru(3)-C(15)	47.0 (2)
Ru(3)-Ru(2)-C(4)	102.5 (3)	Ru(2)-Ru(5)-C(12)	105.9 (3)	Ru(4)-Ru(3)-C(8)	131.1 (3)
Ru(3)-Ru(2)-C(6)	154.2 (3)	Ru(2)-Ru(5)-C(14)	47.5 (2)	Ru(4)-Ru(3)-C(15)	49.9 (2)
Ru(3)-Ru(2)-C(15)	48.8 (2)	Ru(3)-Ru(5)-C(12)	155.0 (3)	Ru(5)-Ru(3)-C(8)	149.7 (3)
Ru(5)-Ru(2)-C(5)	140.1 (3)	Ru(3)-Ru(5)-C(14)	96.1 (2)	Ru(5)-Ru(3)-C(15)	54.4 (2)
Ru(5)-Ru(2)-C(14)	47.6 (2)	Ru(4)-Ru(5)-C(12)	102.3 (3)	Ru(1)-Ru(4)-C(11)	78.6 (3)
Ru(1)-Ru(3)-C(7)	171.6 (2)	Ru(4)-Ru(5)-C(14)	142.8 (2)	Ru(1)-Ru(4)-C(16)	47.5 (2)
Ru(1)-Ru(3)-C(9)	85.2 (2)	Ru(3)-Ru(1)-C(2)	156.4 (2)	Ru(3)-Ru(4)-C(11)	100.6 (3)
Ru(2)-Ru(3)-C(7)	84.1 (2)	Ru(3)-Ru(1)-C(16)	74.6 (2)	Ru(3)-Ru(4)-C(16)	72.8 (2)
Ru(2)-Ru(3)-C(9)	175.0 (2)	Ru(4)-Ru(2)-C(2)	95.2 (2)	Ru(5)-Ru(4)-C(11)	138.3 (3)
Ru(4)-Ru(3)-C(7)	132.4 (2)	Ru(4)-Ru(1)-C(16)	54.5 (2)	Ru(5)-Ru(4)-C(16)	86.9 (2)
Ru(4)-Ru(3)-C(9)	83.4 (2)	Ru(3)-Ru(2)-C(5)	91.5 (3)	Ru(2)-Ru(5)-C(13)	118.6 (2)
Ru(5)-Ru(3)-C(7)	79.0 (2)	Ru(3)-Ru(2)-C(14)	95.1 (2)	Ru(2)-Ru(5)-C(15)	46.3 (1)
Ru(5)-Ru(3)-C(9)	114.8 (2)	Ru(5)-Ru(2)-C(4)	118.9 (3)	Ru(3)-Ru(5)-C(13)	107.0 (2)
Ru(1)-Ru(4)-C(10)	109.3 (3)	Ru(5)-Ru(2)-C(6)	107.0 (3)	Ru(3)-Ru(5)-C(15)	48.3 (1)
Ru(1)-Ru(4)-C(15)	65.6 (2)	Ru(5)-Ru(2)-C(15)	54.1 (2)	Ru(4)-Ru(5)-C(13)	133.1 (2)
				Ru(4)-Ru(5)-C(15)	49.7 (1)
(v) M-M-C					
Ru(2)-C(15)-Ru(3)	84.3 (0)	Ru(1)-C(16)-Ru(4)	77.9 (0)	Ru(3)-C(15)-Ru(5)	77.3 (0)
Ru(2)-C(15)-Ru(5)	79.7 (0)	Ru(1)-C(16)-C(17)	132.2 (3)	Ru(4)-C(15)-Ru(5)	77.3 (0)
Ru(3)-C(15)-Ru(4)	82.8 (0)	Ru(4)-C(16)-C(17)	128.0 (3)	Ru(5)-C(15)-C(16)	142.4 (3)
Ru(3)-C(15)-C(16)	121.1 (3)	Ru(2)-C(15)-Ru(4)	155.6 (0)	Ru(1)-C(16)-C(15)	101.8 (3)
Ru(4)-C(15)-C(16)	73.4 (3)	Ru(2)-C(15)-C(16)	130.9 (3)	Ru(4)-C(16)-C(15)	70.3 (3)
				C(15)-C(16)-C(17)	123.6 (4)

Table VI. Structural Parameters for μ - η -Acetyliides

cluster	acetylide coordinatn	av Ru-C(η), Å	C=C, Å	bend back angle (deg) at		ref
				C α	C β	
Ru ₂ (CO) ₆ (μ -C≡C-t-Bu)(μ - η^2 -C≡C-t-Bu) (μ -PPh ₂) ₂ (PPh ₂ ,C≡C-t-Bu)	μ		1.194 (14)	0	2.1 (6)	22
	μ - η^2	2.456	1.228 (11)	6.5 (3)	16.7 (4)	
Ru ₂ (CO) ₆ (μ - η^2 -C≡C-t-Bu)(μ -PPh ₂)	μ - η^2	2.351	1.218 (4)	21.1 (1)	21.5 (1)	14
Ru ₂ (CO) ₆ (μ_3 - η^2 -C≡C-i-Pr)(μ -PPh ₂)	μ_3 - η^2	2.321	1.284 (8)	26.0 (2)	34.8 (3)	7b
HRu ₃ (CO) ₉ (μ_3 - η^2 -C≡C-t-Bu)	μ_3 - η^2	2.225	1.321 (6)	25.5 (1)	39.8 (2)	23
Ru ₅ (CO) ₁₃ (μ - η^2 -C≡CPh)(μ -PPh ₂)	μ_4 - η^2	2.201	1.342 (11)	0	38.6 (4)	this work
Ru ₅ (CO) ₁₃ (μ -CO)(μ_5 - η^2 -C≡CPh)(μ -PPh ₂)	μ_5 - η^2		1.39 (1)		56.4 (5)	this work

bond. Surprisingly, however, the Ru-P-Ru angle does not differ significantly from that in the dinuclear $\text{Ru}_2(\text{CO})_6$ -

$(\mu-\eta^2\text{-C}\equiv\text{C-}t\text{-Bu})(\text{PPh}_2)$ (72.0 (0)°)¹⁴ where $\delta^{(31)\text{P}}$ appears at +123.9. The exceptionally short Ru(4)-Ru(5) distance

and short Ru-P bond lengths appeared initially to provide a rationale for the low value of $\delta^{31}\text{P}$. However the observation of a ^{31}P shift of 258 ppm for II, where the Ru(4)-Ru(5) and Ru-P bond lengths are not unusual seems to rule out this explanation. The insensitivity of $\delta^{31}\text{P}$ to the changes in bond lengths and angles within the three membered Ru-P-Ru ring may suggest that a major factor contributing to the low-field chemical shifts in these two clusters is the equatorial rather than axial stereochemistry of the phosphido group. We are currently examining this possibility, which may have important ramifications for the structural characterization of phosphido-bridged clusters, in more detail.

Nature of the Adducts in Solution. The demonstration that I undergoes facile addition of CO with metal-metal bond cleavage and skeletal rearrangement and that II readily loses CO to regenerate I suggested that I might be sensitive to other nucleophiles. Evidence for the reversible formation of adducts with MeCN, PhCN, *i*-PrNH₂, *sec*-BuNH₂, and C₅H₅N was obtained from solution IR and ^{31}P NMR studies as well as the isolation of the solid complexes.

Under CO at 263 K solutions of I in THF/CDCl₃ exhibit two ^{31}P resonances at +253.7 ppm (I) and +258.0 ppm (II). The intensities of these resonances changed from 1:2 at 263 K to 1:1 at 293 K as CO was lost from the solution. Above this temperature the peaks began to broaden and the intensity of the +253.7 ppm peak steadily increased.

In the presence of MeCN, solutions of I gave sharp resonances at +253.0 and +258.2 ppm virtually identical with those above. At 308 K these singlets coalesced to a single broad line at +256.1 ppm. Solution infrared spectra of I in MeCN/CHCl₃ showed a bridging $\nu(\text{CO})$ band at 1831 cm⁻¹ similar to that for II (1848 cm⁻¹). The solid adduct also exhibited a bridging $\nu(\text{CO})$ band. While these data are insufficient to unequivocally establish the exact location of the nucleophile, they do suggest that addition of MeCN effects a similar rearrangement of the metal skeleton as CO. Similar spectroscopic features were observed for the adducts with PhCN, *i*-PrNH₂, *sec*-BuNH₂, and C₅H₅N. No reaction was observed with secondary or tertiary aliphatic amines. It is interesting to note that the carbido cluster $\text{Ru}_5(\text{CO})_{15}(\text{C})$ has recently been reported to react with acetonitrile. The adduct $\text{Ru}_5(\text{CO})_{15}\text{C}(\text{MeCN})$ has a structure derived from that of the parent by cleavage of an apical-basal Ru-Ru bond.¹⁹ In the case of I cleavage of a basal-basal Ru-Ru bond appears to be favored.

^{13}C NMR Spectra of I and II. The ^{13}CO NMR spectrum of I at 303 K (Table VII) showed four resonances in the intensity ratios 2:3:6:2 which were assigned on the following basis. The molecule possesses an approximate plane of symmetry (perpendicular to the Ru(1)-Ru(2) bond) such that coordination about Ru(1) and Ru(2) and about Ru(4) and Ru(5) will be identical.²⁷ Intrametallic CO exchange via a trigonal twist mechanism²⁸ at Ru(1) and Ru(2) would thus result in equivalence of six carbonyl ligands (CO(1)-CO(6)). The resonance of intensity 6 at 193.8 ppm is assigned to these ligands. Due to rapid exchange $^2J_{^{13}\text{C}-^{13}\text{C}}$ will not be resolved, in spite of the high enrichment factor. This resonance showed no variation

Table VII. The ^{13}CO NMR Spectra of $\text{Ru}_5(\text{CO})_{13}(\mu_4\text{-}\eta^2\text{-C}\equiv\text{CPh})(\mu\text{-PPh}_2)$ and $\text{Ru}_5(\text{CO})_{14}(\mu_4\text{-}\eta^2\text{-C}\equiv\text{CPh})(\mu\text{-PPh}_2)$

reson	intens	assign ^b
		A. $\text{Ru}_5(\text{CO})_{13}(\mu_4\text{-}\eta^2\text{-C}\equiv\text{CPh})(\mu\text{-PPh}_2)$ ^a
		188 K
202.4	2	C(11), C(13)
197.3	2	C(7), C(9)
195.7	1	C(8)
194.4	6	C(1), C(2), C(3), C(4), C(5), C(6)
191.6	2	C(10), C(12)
		303 K
201.0	2	C(11), C(13)
196.5	3	C(7), C(8), C(9)
193.8	6	C(1), C(2), C(3), C(4), C(5), C(6)
190.7	2	C(10), C(12)
		B. $\text{Ru}_5(\text{CO})_{14}(\mu_4\text{-}\eta^2\text{-C}\equiv\text{CPh})(\mu\text{-PPh}_2)$ ^c
230.3	1	$\mu\text{-CO}$
204.9	1	
199.0	1	
197.6	1	
197.4	1	
195.9	1	
192.0	2	
191.7	2	
190.7	1	
188.9	1	
182.0	1	

^a THF/CDCl₃. ^b For numbering scheme see Figure 1.

^c CD₂Cl₂ at 188 K.

in line shape over the temperature range 188–303 K.

Similarly, rotation of the tricarbonyl unit at Ru(3) will yield a singlet of intensity 3 and the resonance at 196.5 ppm is assigned to these ligands. At 213 K this peak was broad, and at 203 K two broad resonances were observed. At 188 K these were resolved into sharp lines of intensities 2:1 at 197.3 and 195.7 ppm, which are assigned to the symmetry-related pair CO(7) and CO(9) and the unique carbonyl lying in the mirror plane CO(8),²⁹ respectively. We note that the original resonance at 303 K appeared at a population-weighted average position. Full sharpening of these resonances was not observed, and this may be due, in part, to an unresolved $^2J_{^{13}\text{C}-^{13}\text{C}}$.

The dicarbonyl units at Ru(4) and Ru(5) are unable to undergo intrametallic exchange in the absence of bond breaking and exist as mirror-related pairs (CO(10), CO(12) and CO(11), CO(13)).³⁰ In accord with this two resonances of intensity 2 were observed at 201.0 ppm (CO(11), CO(13)) and 190.7 ppm (CO(10), CO(12)) where, in the latter case, the high-field resonance was assigned to the carbonyls trans to metal-metal bonds.³¹ Because of the static nature of these carbonyls coupling to ^{13}C and ^{31}P was observed at 303 K with values $^2J_{^{13}\text{C}-^{13}\text{C}} = 7$ Hz and $^2J_{^{13}\text{C}-^{31}\text{P}}$ (CO(11), CO(13)) = 3 Hz and $^2J_{^{13}\text{C}-^{31}\text{P}}$ (CO(10), CO(12)) ≤ 1 Hz. These values are similar to those found in other systems.³² The line shapes of these resonances were invariant over

(29) It is also possible that the unique carbonyl could be oriented on the opposite side of the cluster, vicinal to the phosphido bridge, rather than on the distal side, as is observed structurally.

(30) Such a process would require rotation of a "tripod" ligand arrangement.²⁸ However, all other substituents at Ru(4) and Ru(5) are in fixed positions.

(31) The chemical shift of equatorial carbonyl ligands in ruthenium clusters, i.e., those trans to metal-metal bonds, are normally observed at higher field. For example: (a) Cotton, F. A.; Hanson, B. E.; Jamerson, J. D. *J. Am. Chem. Soc.* 1977, 99, 6588. (b) Frikott, K. E.; Shore, S. G. *Inorg. Chem.* 1979, 18, 2817. (c) Bryan, E. G.; Forster, A.; Johnson, B. F.; Lewis, J.; Matheson, T. W. *J. Chem. Soc., Dalton Trans.* 1978, 196.

(32) (a) Daresbourg, D. J. *J. Organomet. Chem.* 1981, 209, C37. (b) Aime, S.; Osella, D. *J. Chem. Soc., Chem. Commun.* 1981, 300.

(27) Nonidentical elements in the operation of the mirror plane are the three phenyl substituents, one at C(15) and two at phosphorus. However, barriers to rotation or partial rotation of these groups are expected to be small. This was confirmed in the ^{13}C spectrum of the aromatic carbons at 303 K which showed the 2- and 6-carbon atoms of each ring to be equivalent as well as the 3- and 5-positions. These resonances were only slightly broadened at 188 K.

(28) Johnson, B. F. G. In "Transition Metal Clusters"; Johnson, B. F. G., Ed.; Wiley: New York, 1981; pp 471–543.

the temperature range 188-303 K.

The above assignment and hence the proposed pattern of dynamic behavior for I is inconsistent with that reported for the structurally related carbide clusters $\text{Fe}_4\text{M}(\text{CO})_{x-}(\text{C})$.³³ In the latter systems however intermetallic exchange is rapid at ambient temperature for basal sites although less facile between basal and apical sites; intrametallic exchange at $\text{M}(\text{CO})_3$ units is also facile.

Possible factors contributing to the slow intermetallic exchange in I may include the rigid stereochemistry at Ru(4) and Ru(5), the presence of a $\mu\text{-PPh}_2$ group occupying a site stereochemically equivalent to that of a bridging CO group in one of the proposed intermediates for intermetallic basal ligand exchange in the carbido clusters, and the fact that activation energies for fluxional processes are generally higher for ruthenium than iron clusters. In this regard it is worth noting that whereas the carbonyls bound to the apical atom in the carbido iron clusters appear equivalent at the lowest temperatures attainable,³³ in I rotation of the apical $\text{Ru}(\text{CO})_3$ unit is slow on the NMR time scale at 188 K.

The ^{13}CO spectrum of II (Table VII) did not permit unequivocal assignment of any bands, other than the bridging CO, due to the lack of distinguishing features in the spectrum over the temperature range studied.

Conclusions

The molecule $\text{Ru}_5(\text{CO})_{13}(\mu_4\text{-}\eta^2\text{-C}\equiv\text{CPh})(\text{PPh}_2)$ may be considered as a closed-shell 74-electron cluster according to the EAN rule or as a nido polyhedron with seven skeletal electron pairs in terms of the Wade-Williams-Rudolph-Mingos counting rules.³⁴ In the former case

(33) Tachikawa, U.; Gurts, R. L.; Muetterties, E. L. *J. Organomet. Chem.* 1981, 213, 11.

(34) (a) Wade, K. *Adv. Inorg. Chem. Radiochem.* 1976, 18, 1. (b) Williams, R. E. *Ibid.* 1976, 1, 18. (c) Rudolph, R. W. *Acc. Chem. Res.* 1976, 9, 446. (d) Mingos, D. M. P. *J. Chem. Soc., Dalton Trans.* 1974, 133.

addition of two electrons to give a 76-electron species should result in a polyhedron with only seven metal-metal bonds. In the latter a conversion from a nido octahedron to an arachno pentagonal bipyramid is predicted. Extensions of the skeletal electron counting scheme to include certain hydrocarbon atoms as vertices^{34,35} are not as readily applicable in that, while I can indeed be viewed as a mononapped square pyramid, the CO adduct II does not readily fit into the nido category.

Rearrangements of the type encountered here are fundamental to cluster chemistry. There are, for example, increasing indications that associative interactions may be responsible for ligand exchange and substitution in cluster systems.³ Clearly, cluster metal-metal bond cleavage creating additional coordination sites may play a similar role to the generation of coordinatively unsaturated species in mononuclear chemistry. Exploitation of this behavior in cluster catalysis may be possible.

Acknowledgment. We thank the Natural Sciences and Engineering Research Council of Canada for a grant (A.J.C.) and a scholarship (S.A.M.).

Registry No. I, 85957-32-0; II, 85957-33-1; $\text{Ru}_5(\text{CO})_{13}(\text{C}\equiv\text{CPh})(\text{PPh}_2)(\text{MeCN})$, 85957-34-2; $\text{Ru}_5(\text{CO})_{13}(\text{C}\equiv\text{CPh})(\text{PPh}_2)\text{-}(\text{Pr-}i\text{-NH}_2)$, 85957-35-3; $\text{Ru}_5(\text{CO})_{13}(\text{C}\equiv\text{CPh})(\text{PPh}_2)(\text{sec-BuNH}_2)$, 85957-36-4; $\text{Ru}_5(\text{CO})_{13}(\text{C}\equiv\text{CPh})(\text{PPh}_2)(\text{C}_5\text{H}_5\text{N})$, 85957-37-5; $\text{Ru}_5(\text{CO})_{13}(\text{C}\equiv\text{CPh})(\text{PPh}_2)(\text{PhCN})$, 85957-38-6.

Supplementary Material Available: Table S1, anisotropic thermal parameters for $\text{Ru}_5(\text{CO})_{13}(\mu_4\text{-}\eta^2\text{-C}\equiv\text{CPh})(\mu\text{-PPh}_2)$, Table S2, anisotropic thermal parameters for $\text{Ru}_5(\text{CO})_{14}(\mu_5\text{-}\eta^2\text{-C}\equiv\text{CPh})(\mu\text{-PPh}_2)$, Table S3, additional bond angles and bond lengths for $\text{Ru}_5(\text{CO})_{13}(\mu_4\text{-}\eta^2\text{-C}\equiv\text{CPh})(\text{PPh}_2)$, and Table S4, additional bond angles and bond lengths for $\text{Ru}_5(\text{CO})_{14}(\mu_5\text{-}\eta^2\text{-C}\equiv\text{CPh})(\text{PPh}_2)$, and tables of observed and calculated structure factors for $\text{Ru}_5(\text{CO})_{13}(\mu_4\text{-}\eta^2\text{-C}\equiv\text{CPh})(\mu\text{-PPh}_2)$ and $\text{Ru}_5(\text{CO})_{14}(\mu_5\text{-}\eta^2\text{-C}\equiv\text{CPh})(\mu\text{-PPh}_2)$ (43 pages). Ordering information is given on any current masthead page.

(35) Jaouen, G.; Marinetti, A.; Mentzen, B.; Matin, R.; Saillard, J. Y.; Sayer, B. G.; McGlinchey, M. J. *Organometallics* 1982, 1, 752.

Reactions of 2-Alkoxyfurans with Nonacarbonyldiiron or Dodecacarbonyltriruthenium Giving Binuclear Vinylcarbene Complexes and a 2-Pyrone Complex. A Novel Precursor for α,β -Unsaturated Alkylidene Ligands and an Unusual Carbonylation of the Furans

Take-aki Mitsudo, Yasukazu Ogino, Yukitsu Komiya, Hiroyoshi Watanabe, and Yoshihisa Watanabe*

Department of Hydrocarbon Chemistry, Faculty of Engineering, Kyoto University, Sakyo-ku, Kyoto 606, Japan

Received December 2, 1982

2-Methoxyfuran reacted with nonacarbonyldiiron in diethyl ether at 35 °C for 4 h to give a binuclear α,β -unsaturated alkylidene complex, hexacarbonyl(μ -3- η^1 -anti-(methoxycarbonyl)- η^3 - η^1 -allyl)diiron(Fe-Fe) (5a) and a 2-pyrone derivative, tricarbonyl(3-6- η -6-methoxy-2-pyrone)iron (6a). 2-Methoxyfuran also reacted with dodecacarbonyltriruthenium in benzene under an atmosphere of carbon monoxide at 150 °C for 4 h to give a corresponding binuclear α,β -unsaturated alkylidene complex, hexacarbonyl(μ -3- η^1 -anti-(methoxycarbonyl)- η^3 - η^1 -allyl)diruthenium(Ru-Ru) (10), 6-methoxy-2-pyrone (11), and dimethyl glutamate (12). Both reactions could be explained by assuming mononuclear η^3 -vinylcarbene complexes as reaction intermediates.

Much attention has been focused on the chemistry of alkylidene-transition-metal complexes; mono- (1)¹ and

binuclear (2)² alkylidene complexes have been well investigated especially concerning the mechanism for